Geochemistry, Geophysics, Geosystems®

AGU ADVANCING EARTH AND SPACE SCIENCE

RESEARCH ARTICLE
10.1029/2021GC010090

Slow Slip Triggers the 2018 M_w 6.9 Zakynthos Earthquake Within the Weakly Locked Hellenic Subduction System, Greece

Vasso Saltogianni[1], Vasiliki Mouslopoulou[2], Armin Dielforder[1,3], Gian Maria Bocchini[4], Jonathan Bedford[1], and Onno Oncken[1]

[1]GFZ Helmholtz Centre Potsdam, German Research Centre for Geosciences, Potsdam, Germany, [2]National Observatory of Athens, Institute of Geodynamics, Athens, Greece, [3]Institute of Geology, Leibniz University Hannover, Hannover, Germany, [4]Ruhr University of Bochum, Institute of Geology, Mineralogy and Geophysics, Bochum, Germany

Abstract Slow slip events (SSEs) at subduction zones can precede large-magnitude earthquakes and may serve as precursor indicators, but the triggering of earthquakes by slow slip remains insufficiently understood. Here, we combine geodetic, Coulomb wedge and Coulomb failure-stress models with seismological data to explore the potential causal relationship between two SSEs and the 2018 M_w 6.9 Zakynthos Earthquake within the Hellenic Subduction System. We show that both SSEs released up to 10 mm of aseismic slip on the plate-interface and were accompanied by an increase in upper-plate seismicity rate. While the first SSE in late 2014 generated only mild Coulomb failure stress changes (≤3 kPa), that were nevertheless sufficient to destabilize faults of various kinematics in the overriding plate, the second SSE in 2018 caused stress changes up to 25 kPa prior to the mainshock. Collectively, these stress changes affected a highly overpressured and mechanically weak forearc, whose state of stress fluctuated between horizontal deviatoric compression and tension during the years preceding the Zakynthos Earthquake. We conclude that this configuration facilitated episodes of aseismic and seismic deformation that ultimately triggered the Zakynthos Earthquake.

Key Points:

- Two slow-slip events (each ≤10 mm) on the plate-interface of the western Hellenic subduction system are explored
- Stress perturbations due to slow-slip promoted failure of upper-plate faults and triggered the 2018 M_w 6.9 Zakynthos Earthquake
- The forearc is mechanically weak and small friction changes on the megathrust with time, may reverse the stress-state in the upper-plate

Supporting Information:

Supporting Information may be found in the online version of this article.

Correspondence to:

V. Saltogianni,
salto@gfz-potsdam.de

Citation:

Saltogianni, V., Mouslopoulou, V., Dielforder, A., Bocchini, G. M., Bedford, J., & Oncken, O. (2021). Slow slip triggers the 2018 M_w 6.9 Zakynthos Earthquake within the weakly locked Hellenic Subduction System, Greece. *Geochemistry, Geophysics, Geosystems*, *22*, e2021GC010090. https://doi.org/10.1029/2021GC010090

Received 9 AUG 2021
Accepted 21 OCT 2021

1. Introduction

Over the last two decades, an increasing body of evidence shows that subduction megathrusts, in addition to breaking due to large-magnitude (M > 7) earthquakes or creeping aseismically, may also release strain through slow slip events (SSEs) (Dragert et al., 2001; Heki et al., 1997; Hirose et al., 1999; Ohta et al., 2006; Radiguet et al., 2012; Uchida et al., 2016; Wallace & Beavan, 2010). This occurs when the plate-interface slips at rates lower than those required to generate seismic energy (Heki et al., 1997), often releasing, over time periods of days to years, seismic moment equivalent to earthquakes of M_w 6–7.5 (Dragert et al., 2001; Peng & Gomberg, 2010). SSEs mainly occur around the downdip and updip limits of the seismogenic zone, which typically characterize regions of the megathrust that are dominated by conditionally stable friction (Scholz, 1998; Schwartz & Rokosky, 2007). Evidence of SSEs has been observed in a wide range of tectonic regimes and at different stages of the earthquake cycle, associated mainly with fluctuations in pore fluid pressure, frictionally weak materials and the stress-state of the fault (Bürgmann, 2018).

The release of strain through SSEs can transfer stress to the seismogenic zone capable of triggering large-magnitude (M > 6) earthquakes (Bouchon et al., 2013; Cruz-Atienza et al., 2021; Mazzotti & Adams, 2004; Segall & Bradley, 2012). On the other hand, seismic moment released episodically through one or more SSEs may also delay earthquake rupture or result in numerous smaller-sized (M < 6) earthquakes (Dixon & Moore, 2007; Obara & Kato, 2016; Radiguet et al., 2012). Thus, exploring the role of aseismic deformation in triggering large-magnitude earthquakes is crucial for better quantifying time-dependent seismic hazard.

The factors that control the duration and spatial extent of aseismic deformation over the earthquake cycle are still not well understood, mainly due to limited data. This issue is amplified in cases in which slow slip occurs within complex tectonic settings that include faults of various kinematics and slip rates. Such settings often typify terminations of active subduction zones, where plate-motion is partitioned between the plate-interface and the overriding plate, producing complex fault and rupture patterns (Mann &

Frohlich, 1999; Mouslopoulou et al., 2019, 2020; Wallace et al., 2012). The October 25, 2018 M_w 6.9 Zakynthos Earthquake in Greece (Figure 1), provides a rare example of a composite earthquake that ruptured a subduction termination following the synergy of SSEs, earthquake swarms and fault interactions (Figure 1) (Mouslopoulou et al., 2020).

The Zakynthos mainshock is characterized by an oblique mechanism, with a significant non double-couple component (Figure 1) that results from slip on two individual fault sources: a thrust and a strike-slip (Mouslopoulou et al., 2020; Sokos et al., 2020). Decomposition of this moment tensor (Mouslopoulou et al., 2020) suggests a relatively steep dip angle (~45°) for the thrust subevent, which could be compatible with a splay-thrust fault (Cirella et al., 2020; Mouslopoulou et al., 2020). Although there is an ongoing debate as to whether the thrust component of slip was accommodated by a splay-thrust fault or the plate-interface itself (Cirella et al., 2020; Ganas et al., 2020; Mouslopoulou et al., 2020; Sokos et al., 2020), we favor the former scenario as it is supported by: (a) seismic reflection and bathymetric data that reveal numerous NNW-SSE trending thrusts that dip 30°–50° to the northeast, beneath Zakynthos and western Peloponnese (Mouslopoulou et al., 2020 and references therein; Figure S1 in Supporting Information S1), (b) the recording of a minor tsunami along the western coastline of Peloponnese that suggests displacement of the sea-bed (Cirella et al., 2020), and (c) the thrust focal mechanisms resolved for a cluster of aftershocks north of the mainshock hypocenter that mainly span depths of 5–15 km (Figure S1 in Supporting Information S1) (Mouslopoulou et al., 2020).

The SSEs that preceded the 2018 Zakynthos Earthquake were the first to be reported within the Hellenic Subduction System (HSS) and are thought to be responsible for ~4 years of tectonic unrest leading up to the M_w 6.9 mainshock (Figure 1) (Mouslopoulou et al., 2020). Nevertheless, the causal relationship between the SSEs and the 2018 mainshock, as well as the mechanical state of the forearc that hosted this tectonic unrest, remain unexplored and are the foci of this paper. Here, we combine geodetic, Coulomb wedge and Coulomb failure-stress models with earthquake statistics to quantitatively show that both SSEs occurred on the plate-interface at depths ranging from 15 to 40 km and caused stress perturbations capable of gradually "unlocking" the mechanically fragile Hellenic forearc and trigger the 2018 Zakynthos Earthquake. These findings may be important for other weakly locked subduction margins worldwide.

2. Results

2.1. GPS Transient Signals

Mouslopoulou et al. (2020) reported the occurrence of two long-lived (~5 months each) transient signals beneath western Peloponnese during the ~4 years preceding the 2018 Zakynthos Earthquake on the basis of GPS observations (Figure 1b, Figure S2 in Supporting Information S1). The first recorded transient occurred from September 2014 to March 2015 and was followed by a clear drop in the b-value (Mouslopoulou et al., 2020) within the study area (Figure 1c). The second occurred during the ~5 months preceding the Zakynthos mainshock (Figure 1c). Transients comprised successive phases of landward and trenchward acceleration (of ~2–3 months each), with the trenchward motion revealing SSEs at depth (Figure 1c; Mouslopoulou et al., 2020). The tectonic origin of these transient signals was extensively tested against hydrological and seasonal effects, reference-frame errors and different processing codes (see Supporting Information S1 in Mouslopoulou et al. [2020]). Evidence of a transient signal in northwest Peloponnese in May 2018, is also reported by Briole et al. (2021).

The transient signals, reported by Mouslopoulou et al. (2020), were recovered from the median of a total of 250 trajectory models, using the Greedy Automatic Signal Decomposition algorithm (GrAtSiD) (Bedford & Bevis, 2018). This algorithm decomposes, using a linear regression, the GPS signal into (a) the seasonal oscillation signal; (b) the secular and transient motions, and (c) the residual (noise) signal. Our analysis shows that the average noise ranges between 1–2 and 3–5 mm for the horizontal and vertical components, respectively. Therefore, the Signal/Noise ratio (SNR) of the largest detected horizontal transients in Zakynthos Island and northwest Peloponnese (Figure 1b) ranges between 1 and 4, indicating that, at least, the largest values in the observed displacement gradient (Figure 1b) are above the GPS noise level. Furthermore, power spectrum analysis of the GPS noise signal of the final trajectory model across all stations, shows that the noise signal is dominated by white noise (Gaussian noise) at higher frequencies (for $f > \sim 10^{-2}$ 1/day, that

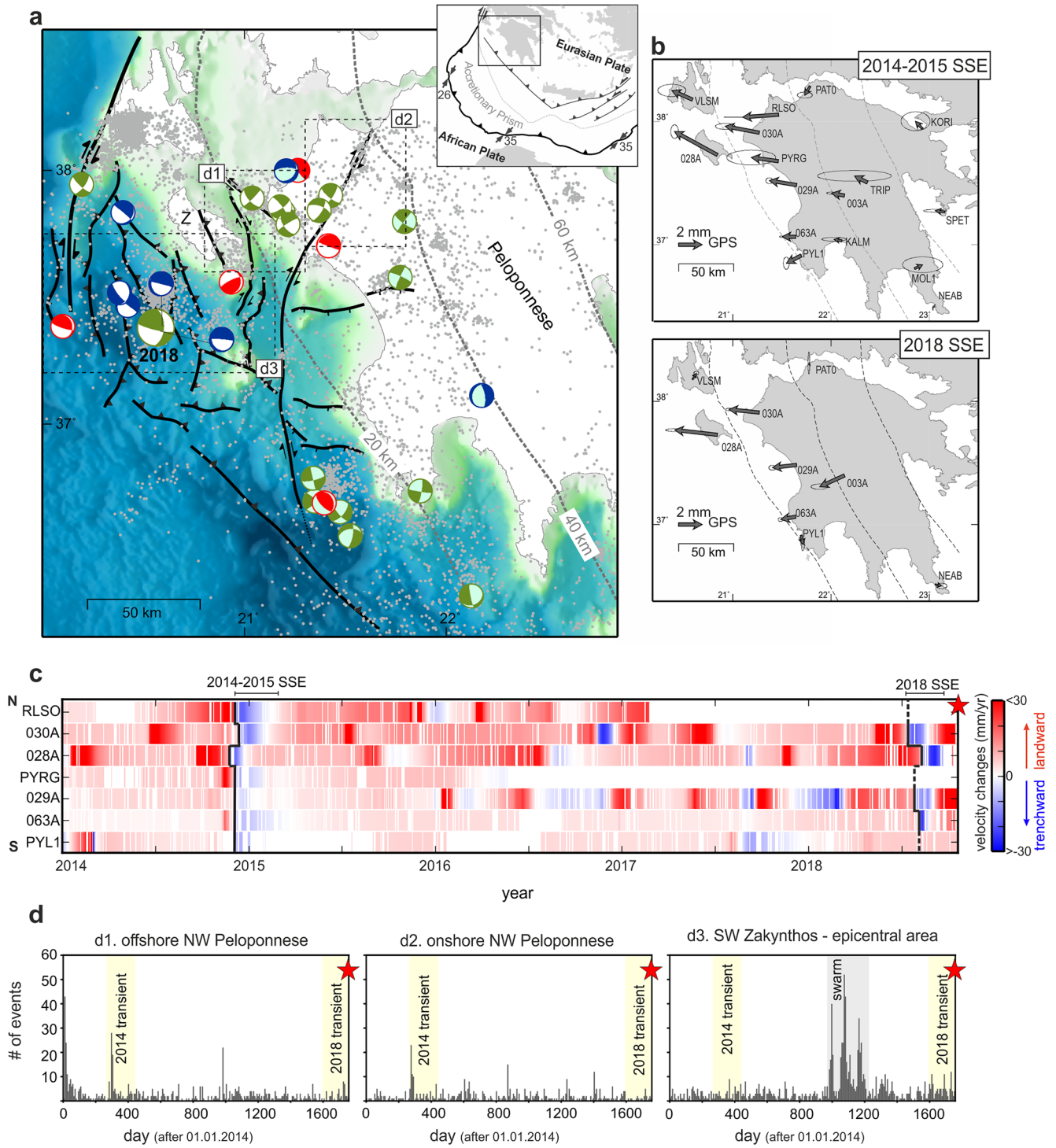

Figure 1. Summary of the 4-year long preparatory phase of the 2018 Zakynthos Earthquake. (a) Map of the study area summarizing the 2018 Zakynthos mainshock (large green beachball) and focal mechanisms of the M > 4 earthquakes that occurred during the preparatory phase (red: reverse, green: strike-slip, blue: normal) (Mouslopoulou et al., 2020; white filling) (NOA repository; cyan filling). Offshore faulting is modified from Mouslopoulou et al. (2020). Relocated seismicity is denoted by gray dots (M ≥ 2). Depth contours of the top of the plate-interface are indicated by gray dashed lines (Halpaap et al., 2019). Inset: The study area is located at the western termination of the Hellenic Subduction System (HSS). Z = Zakynthos Island. (b) Cumulative trenchward transient displacements as derived from Mouslopoulou et al. (2020) for the 2014–2015 and 2018 SSEs, together with their uncertainties (1-sigma). (c) Spatiotemporal evolution of daily velocities along the east component of near-field GPS stations from south to north. (e) Histograms of the number of events as a function of time within areas d1-d3 in (a). The end of the *x*-axes in (c and d) marks the timing of the 2018 Zakynthos Earthquake (red star).

is, $T < \sim$100 days) (Figure S3 in Supporting Information S1). Given the assumption that the non-tectonic, non-seasonal noise has a Gaussian (white) distribution, the recovery of Gaussian residuals by the GrAtSiD trajectory model in this case indicates an appropriate fitting of the time series (Bedford & Bevis, 2018) for the frequencies of interest (2–3 months long). Accordingly, under- or over-fitting of the time series would be indicated by a residual with flicker (pink) noise spectral characteristics (Bedford & Bevis, 2018). While a flicker noise spectrum is commonly assumed to be the dominant noise signature in GNSS displacement time series (Dmitrieva et al., 2015; Langbein, 2008), it was demonstrated in Bedford and Bevis (2018) that this assumption could be an artifact of signal decomposition in which tectonic and seasonal signals leak into the assumed noise portion of the signal, and that an assumption of Gaussian noise is just as valid as an assumption of flicker noise for the non-seasonal, non-tectonic portion of the signal. Thus, this analysis demonstrates that the detection of transients by Mouslopoulou et al. (2020) is clearly above the data noise level.

2.2. Geodetic Modeling of the Slow Slip Events (SSEs)

Here, we adopt the cumulative GPS displacements derived by Mouslopoulou et al. (2020) for the trenchward phase of the transient signal (Figure 1b; Figure S2 in Supporting Information S1), to constrain the spatial extent and size of the two SSEs. We invert the GPS displacements (Figure 2) for variable distributed slip at depth, assuming an elastic homogeneous half-space (Okada, 1985) and using the SDM2011 software (Wang et al., 2009). The modeled geometries of the plate-interface and upper-plate faults were constrained by combining data from seismic tomography (Halpaap et al., 2018, 2019), seismicity distribution (Bocchini et al., 2018), moment tensors and analysis of seismic reflection profiles (Mouslopoulou et al., 2020).

After testing for various kinematic scenarios, including synchronous slip on the plate-interface and upper-plate faults (Text S1 in Supporting Information S1), we derive our preferred model which resolves for transient aseismic slip on the plate-interface (Figure 2). Both the 2014–2015 and 2018 SSEs show similar spatial distribution patterns that involve slow slip extending (a) along western Peloponnese at plate-interface depths of ~20–40 km and (b) between west of Zakynthos Island and NW Peloponnese at shallower plate-interface depths (~15–20 km) (Figures 2a and 2b). We obtain average slip of 3 and 4 mm for the 2014–2015 and 2018 SSEs, respectively. The 2014–2015 transient is associated with locally maximum slip of 9 mm at depths of ~25 km (offshore NW Peloponnese) whereas maximum slip of 10 mm is modeled for the 2018 transient at depths of ~30 km beneath western Peloponnese (Figure 2). The total geodetic moment released by the SSEs is 4.3×10^{18} Nm (2014–2015 SSE) and 3.8×10^{18} Nm (2018 SSE), corresponding, for each SSE, to an earthquake of M_w 6.4, consistent with results in Mouslopoulou et al. (2020). Both, the duration and the geodetic moment associated with each modeled SSE plot, in agreement with other SSEs reported globally (Figure S9 in Supporting Information S1) (Peng & Gomberg, 2010).

The downdip extent of aseismic slip is also constrained by the distribution of vertical displacements which, despite their significant uncertainties, clearly indicate a change in their polarity, from broad uplift west of the ~40 km plate-interface isodepth to broad subsidence east of it (Figure 2c). This reversal in the polarity of the vertical motion has been recognized in other subduction systems to straddle the rheological boundary from stick-slip to creep (i.e. Wallace & Beavan, 2006). Hence, combining this information (i.e., reversal in the vertical motion and no slip at depths greater than 40 km) we constrain the frictional-to-viscous transition zone beneath western Peloponnese at ~30–40 km depth. The updip extent of the SSEs is modeled at a depth of ~15 km, extending beneath the island of Zakynthos and western Peloponnese.

Although our analysis suggests that aseismic slip is released on the plate-interface and explains most of the geodetic signal through this scenario (Figure 2), an alternative scenario in which aseismic slip may be also partly accommodated on upper-plate faults cannot be excluded (see Figures S7 and S8 in Supporting Information S1) (Bürgmann, 2018; Hamling & Wallace, 2015; Mouslopoulou et al., 2020; Shaddox & Schwartz, 2019). This is also consistent with the recorded obliquity between the observed and modeled (Figure 2a) displacement vectors during the 2014–2015 SSE (Mouslopoulou et al., 2020). Indeed, modeling suggests that this slip scenario (synchronous slow slip on the plate-interface and upper-plate faults) fits equally well the observations (Text S1 in Supporting Information S1). By contrast, the spatiotemporal resolution of the available geodetic data does not allow the detection of any clear migration of aseismic slip along the margin (e.g., in an approximately N-S orientation) (Figure 1b).

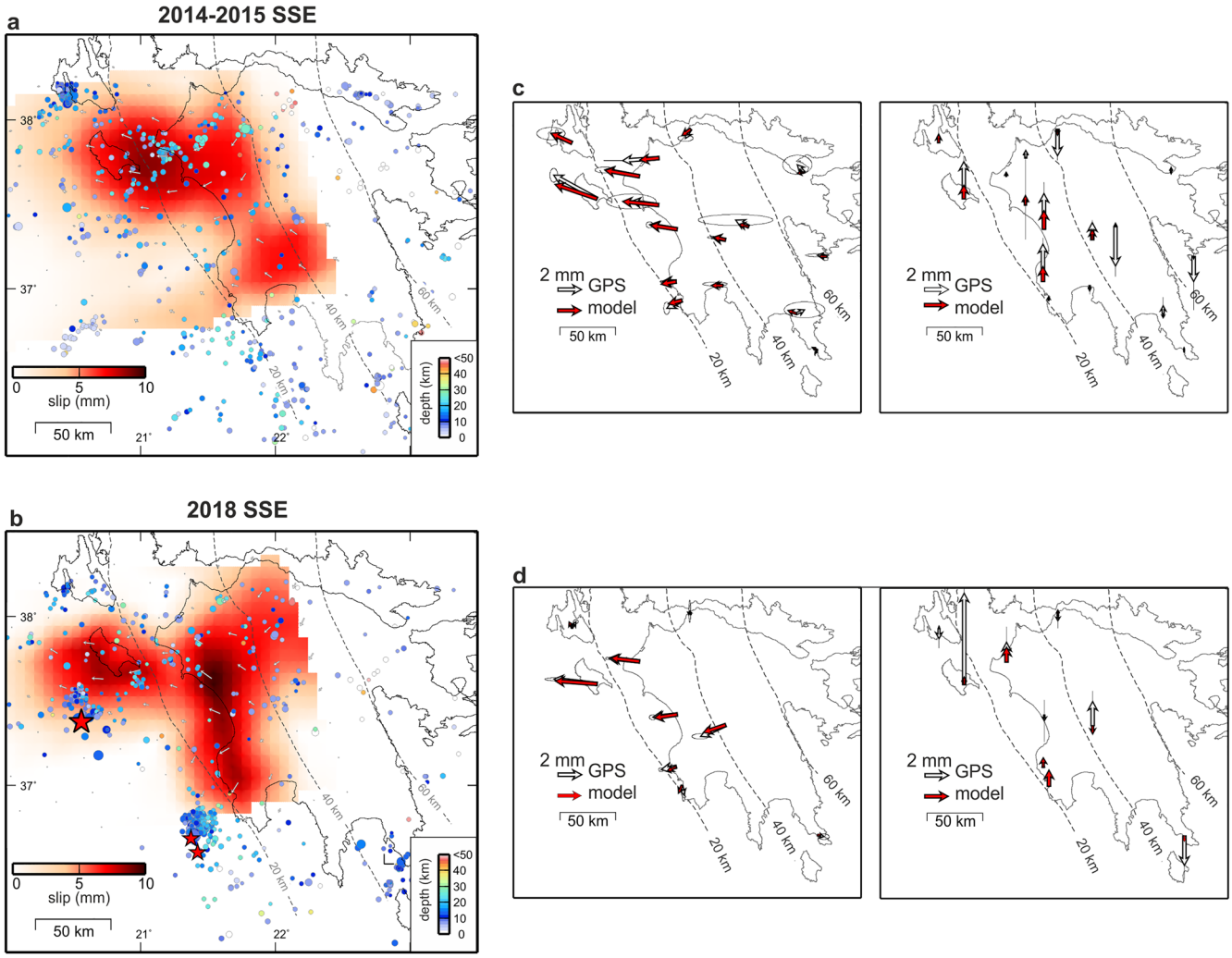

Figure 2. The modeled distribution of the 2014–2015 (a) and 2018 (b) SSEs on the Hellenic plate-interface. Color-coded filled circles indicate microseismicity during the two SSEs while red stars denote the M_w 6.9 Zakynthos mainshock (north) and the two M > 5 events offshore SW Peloponnese (south) in 2018. (c and d) Measured (white arrows) and modeled (red arrows) horizontal and vertical GPS displacements corresponding to the models illustrated in (a and b), respectively. Error ellipses depict 1-sigma uncertainty.

2.3. Changes in Seismicity Rates

Apparent changes in seismicity rates in the forearc are evident during the two transient episodes in northwest Peloponnese and the epicentral area (Figure 1d). For this reason, here we investigate possibly statistically significant changes in the seismicity rates in response to the two SSEs after we updated and extended the relocated seismic catalog of Mouslopoulou et al. (2020). The revised catalog includes a total of 20,289 events that occurred between January 1, 2014 and October 25, 2018 over latitude and longitude ranges of between 36°–38.2°N and 19°–23.5°E, respectively (Data Set S1; Text S2 in Supporting Information S1). Seismicity is primarily confined within the upper-plate (<20–25 km) and includes mostly events of magnitude M_L < 3.5 (Figures S12 and S13 in Supporting Information S1). To identify potential changes in the rates of seismicity due to the recorded geodetic transients, we performed two standard statistical tests: the β- and *Z*-statistic (Marsan & Wyss, 2011). These tests quantify the changes in seismicity rates before and after a stressing event, that is, here the geodetic transient events. Specifically, the β-statistic quantifies changes in the seismicity rates by comparing the number of events before and after each stressing event while the final score is normalized only by the number of events preceding the stressing event (Matthews & Reasenberg, 1988). The Z-statistics (Habermann, 1981) is a more symmetric version of the β-statistic (Marsan & Wyss, 2011), as the final score is normalized by the number of events that precede and follow the stressing

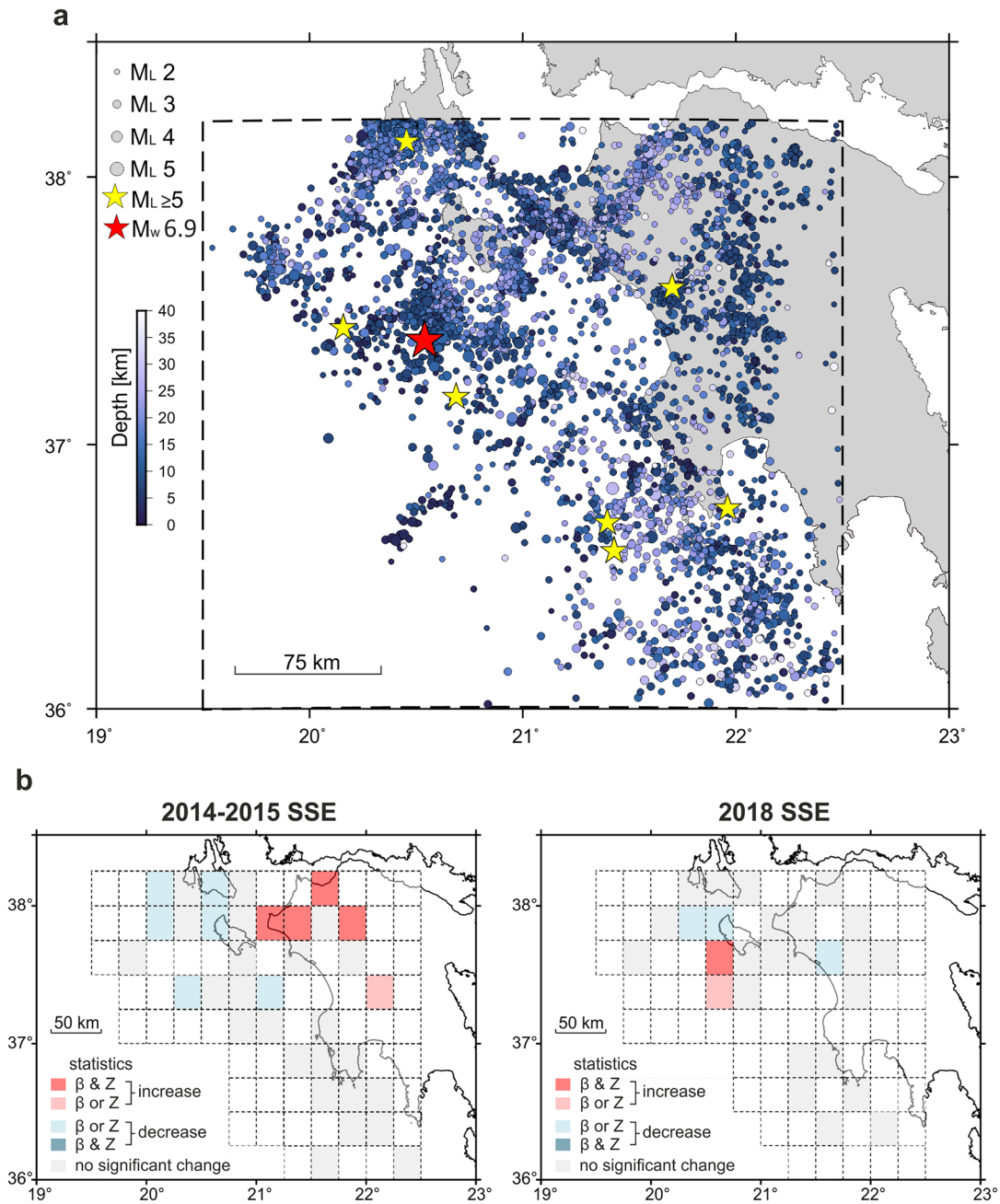

Figure 3. Changes in seismicity rates during the transient episodes. (a) Map-view of the relocated seismicity for the period January 1, 2014 to October 25, 2018 ($M_L \geq 2$ and depth ≤ 40 km) (b) *β*- and *Z*- earthquake statistics associated with the SSEs. Regions with significant increases (red) and decreases (blue) in seismicity rates, before and after the onset of the geodetic transients, are highlighted. Cells with no significant change and with <10 events are highlighted gray and white, respectively.

event—this test is particularly reliable when the total number of events is low. For the purpose of these statistical tests, we filtered out events with magnitudes $<M_c = 2$ and hypocentral depths >40 km. We have also declustered the initial catalog by removing all aftershocks associated with the two $M_w > 5$ earthquakes that occurred offshore SW of Peloponnese during the 2018 transient (Figure 3a and Figure S14; Text S3 in Supporting Information S1). The statistical tests were performed on the filtered catalog (6,601 events) and on an equally spaced grid with dimensions of 0.25° × 0.25° (Figure 3b).

Our analysis shows that during the 2014–2015 transient, there is an increase in the rate of seismicity in northwest Peloponnese (Figure 3b). This change occurs at depths ranging from about 5 to 25 km (Figures S12–S14 in Supporting Information S1) and is here thought to be associated with slip on two steep strike-slip faults onshore (dextral) and offshore (sinistral) NW Peloponnese as jointly suggested by analysis of moment tensors and seismic reflection profiles (Haddad et al., 2020; Mouslopoulou et al., 2020) (Figure 1a). No other significant changes are observed. The second geodetic transient, immediately preceding the main-shock, is associated with a significant increase in the seismicity rates in the epicentral region of the M_w 6.9 earthquake (Figure 3b; Figures S12 and S14 in Supporting Information S1). This analysis quantitatively confirms the results of Mouslopoulou et al. (2020) for increased upper-plate microseismicity associated with the transient deformational events.

2.4. Mechanical Stability of the Western Hellenic Forearc

To evaluate the mechanical stability of the western Hellenic forearc we determined the effective strength of the forearc crust and the Hellenic megathrust using the dynamic Coulomb wedge theory (Wang & Hu, 2006). This theory simplifies the wedge-shaped forearc, in a cross-section normal to the plate margin (Figure 4a), as a material of elastic–perfectly Coulomb plastic rheology. Given the wedge geometry, the mechanical stability of the wedge is a function of the effective strength of the megathrust μ'_b, and the effective strength of the wedge material $\mu'_w = \mu(1-\lambda)$, where μ is the coefficient of friction of the wedge material and λ is the pore fluid pressure ratio within the wedge. Depending on the values of μ'_b and μ'_w, the wedge can be in a mechanically stable state, at which it deforms only elastically, or in a critical state, at which it fails by faulting (Figure 4b). Higher values of μ'_b increase the compression of the wedge and promote reverse faulting (compressively critical state in Figure 4b), while lower values of μ'_b decrease the compression of the wedge and promote normal faulting (extensionally critical state). Accordingly, the occurrence of reverse and normal faulting events provides an upper and lower bound of both μ'_b and μ'_w values, respectively (Dielforder, 2017; Wang & Hu, 2006; Wang et al., 2019). We note that the conditions for strike-slip faulting are not directly determined by the Coulomb wedge analysis, as out-of-plane stresses are not considered, but fall within the limits constrained by the compressively and extensionally critical states.

We applied the dynamic Coulomb wedge model to the forearc east (inner wedge) and west (outer wedge) of the Zakynthos Island, respectively (Figure 4a). As illustrated in Figure 1a and Figure S1 in Supporting Information S1, both areas accommodate simultaneous reverse, strike-slip and normal faulting at average depths of ~≤10 km (including also the years preceding the 2018 Zakynthos earthquake) (Mouslopoulou et al., 2020), indicating that the stress state in the Hellenic forearc varies between horizontal deviatoric compression and tension. For the inner wedge, normal faulting requires a very weak megathrust with $\mu'_b \leq 0.01$ and near lithostatic pore fluid pressures with $\lambda \approx 0.95$, which translates to an effective strength of the wedge of $\mu'_w \approx 0.02$ (Figure 4b). For this strength of the wedge, reverse faulting takes place if the megathrust is slightly stronger ($\mu'_b \geq 0.02$). By comparison, normal faulting in the outer wedge requires $\mu'_b \leq 0.04$ and suggests an effective strength of the wedge $\mu'_w \approx 0.06$ (Figure 4b). For this wedge strength, reverse faulting occurs if $\mu'_b \geq 0.05$.

Overall, the dynamic Coulomb wedge analysis shows that the effective strength of the Hellenic megathrust is very low and becomes almost negligible underneath the inner wedge (Figure 4c). The average strength of $\mu'_b \approx 0.03 \pm 0.03$ is consistent with the strength of other subduction megathrust worldwide, which typically is about 0.03 (Gao & Wang, 2014; Lamb, 2006). Moreover, the reverse and normal faulting east and west of Zakynthos requires that the effective strength of the forearc crust to be as low as the one of the megathrust. At these conditions, small changes in megathrust friction suffice to change the mechanical state of the forearc from stable to compressively or extensionally critical. Therefore, our findings support a diverse style of faulting over small spatial scales in the western HSS arising from small spatial heterogeneities in the megathrust friction. This is in agreement with Mouslopoulou et al. (2020) where a mixture of strike-slip, normal, and reverse earthquakes were recorded prior (Figure 1a) and after the 2018 Zakynthos mainshock and also consistent with variable crustal stress field inferred from inversion of earthquake focal mechanisms (Konstantinou et al., 2017).

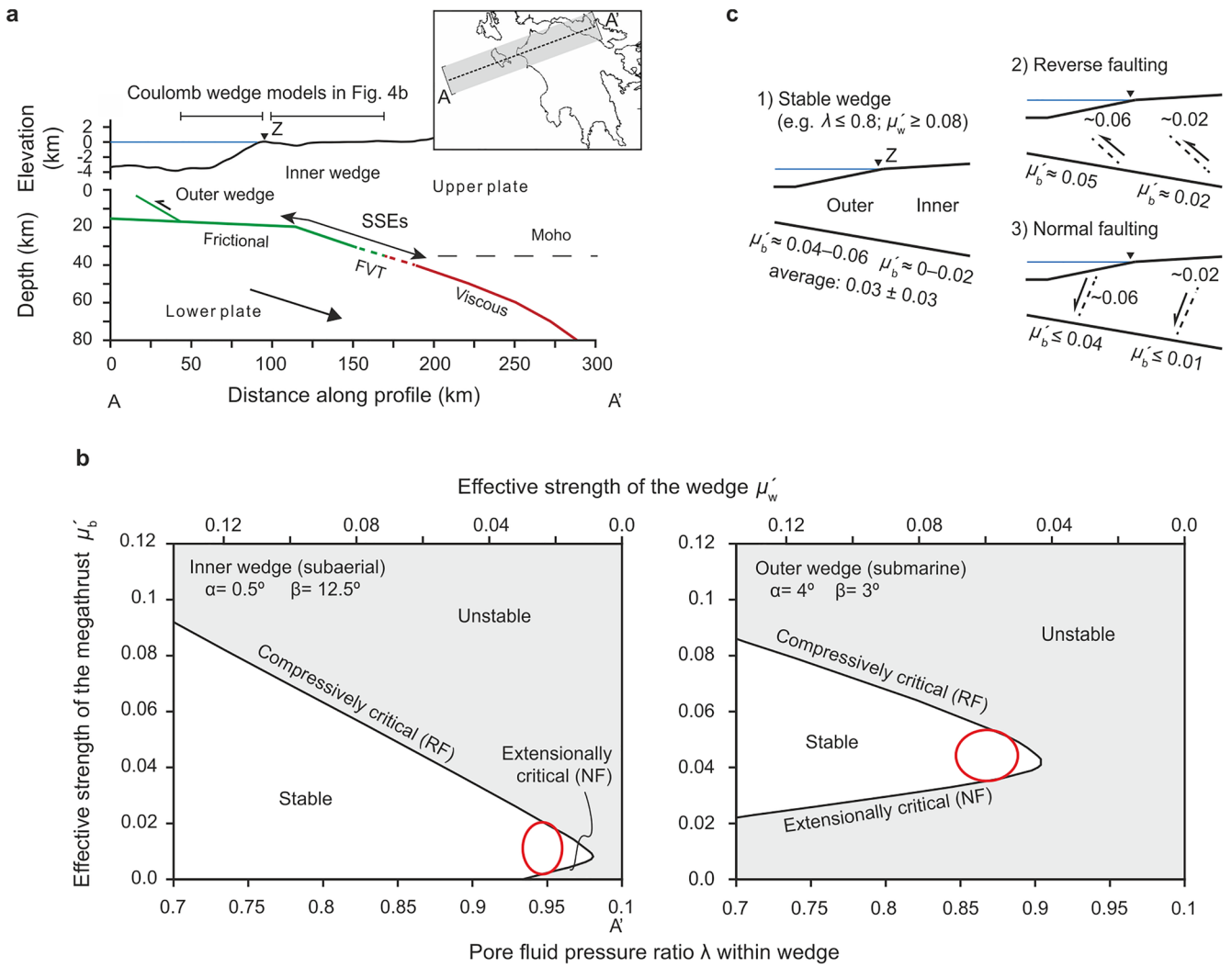

Figure 4. Fault strength and faulting conditions in the Hellenic forearc. (a) Schematic cross-section across the HSS along a 50-km-wide swath profile (inset map). *Z*, Zakynthos Island. The plate-interface comprises an upper frictional segment (green) and a lower viscous segment (red). The frictional-to-viscous transition (FVT) along the megathrust is at 30–40 km depth. (b) Coulomb wedge models for the inner (mostly subaerial) and outer (submarine) wedge. RF: reverse faulting, NF: normal faulting. Red ellipse illustrates approximate solutions that are consistent with the upper-plate faulting pattern. (c) Sketch summarizing the preferred Coulomb wedge solutions for the effective strength of the megathrust (μ'_b) and the effective strength of the wedge (μ'_w).

2.5. Stress Perturbations in the Forearc Crust

Here, we explore whether the SSEs along the plate-interface promoted failure in the upper-plate prior to the Zakynthos mainshock (Mouslopoulou et al., 2020) and identify the sections of the crust that experienced significant stress increases by calculating the Coulomb Failure Stress changes (ΔCFS) on specific upper-plate receiver faults (Figure 5). ΔCFS predicts changes in shear (τ) and normal (σ) stresses in the direction of movement on a receiver fault due to slip of an adjacent fault. Here, we include into the calculations the results of the strength estimates for upper-plate faults obtained in Section 2.4 and adopt a value of $\mu' = 0.05$ for these faults (Figure 4c). Higher values were also tested and had minimal effect on the results (Figure S16 in Supporting Information S1).

We choose to estimate the stress changes that occurred due to the 2014–2015 SSE along two upper-plate faults (in offshore and onshore NW Peloponnese) which were seismically active during the preparatory phase (Figures 1a and 3) (Mouslopoulou et al., 2020). Using the dip/strike and slip direction presented for these faults in Mouslopoulou et al. (2020), we calculate the Coulomb stress changes at crustal depths of ~10 km (Figures 5a and 5b). Our calculations show that the recorded elevated seismic activity (Figure 3)

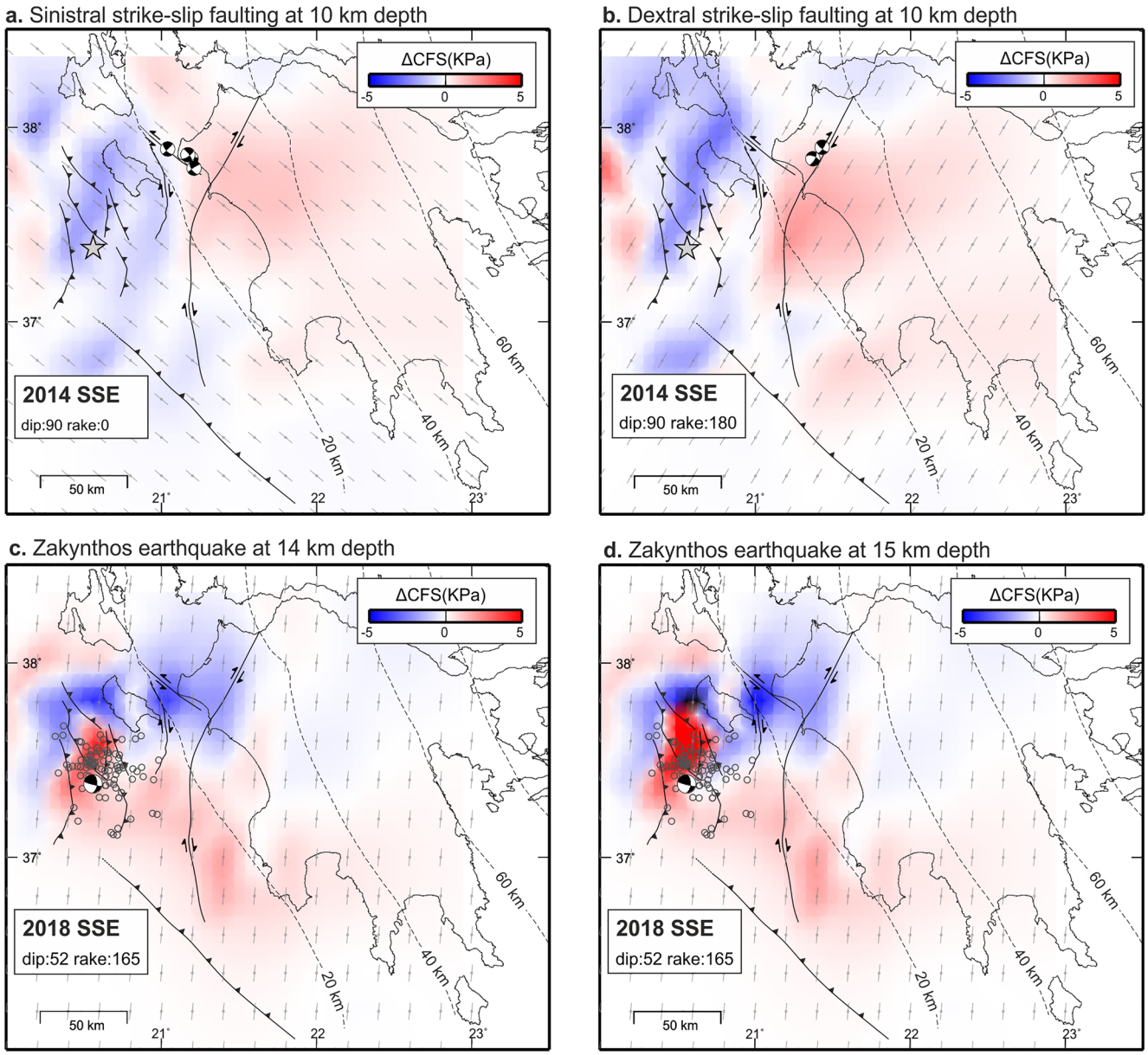

Figure 5. Coulomb failure stress changes (ΔCFS) due to SSEs. ΔCFS in the upper crust (10–15 km) for receiver faults due to slow slip on the plate-interface. The notional strike of each fault is indicated by the patterns of short gray lines whereas the dip/rake is annotated on each map (fault attributes from Mouslopoulou et al. [2020]). (a and b) ΔCFS at 10 km depth tailored to (a) a NW-SE sinistral and (b) a NE-SW dextral strike-slip fault and their associated moment tensors. (c and d) ΔCFS at depths of (c) 14 km and (d) 15 km tailored to the focal mechanism of the 2018 Zakynthos Earthquake. Open circles indicate aftershocks during the first 5 days of the Zakynthos mainshock. Main active faults are also shown. Epicenter of the Zakynthos Earthquake is denoted in (a and b) by gray star.

lies in areas of increased ΔCFS (Figure 5b) or where ΔCFS transition from negative to positive values (Figure 5a). The modeled stress perturbations due to the 2014–2015 SSE reach values up to ~3 kPa at depths of ~10 km.

Following the same procedure, we predict the ΔCFS due to the 2018 SSE (Figures 5c and 5d). Here, the receiver fault is tailored to the characteristics of the moment tensor of the 2018 Zakynthos mainshock (strike:005°, dip:52°, and rake:165°) (Mouslopoulou et al., 2020). In this case, we explore the ΔCFS at two indicative crustal depth profiles, that of 14 and 15 km, to account for uncertainties in the estimation of the earthquake's hypocenter (14 ± 4 km depth) (Mouslopoulou et al., 2020) and in the plate-interface geometry

(Halpaap et al., 2018, 2019). Results, summarized in Figures 5c and 5d, indicate that the 2018 M_w 6.9 Zakynthos Earthquake, together with its early aftershock sequence (≤5 days), is clearly located within a region of the crust that has experienced stress increases up to 25 kPa. The distribution of the ΔCFS is in very good agreement with the observed changes (increases and decreases) in the seismicity rates proximal to the epicentral area (Figures 3b, 5c, and 5d).

Hence, ΔCFS modeling suggests that stress changes as small as ~3 kPa may be capable (Cochran et al., 2004; Harris, 1998; King et al., 1994; Reasenberg & Simpson, 1992) of destabilizing the overriding plate over multiple fault orientations. It also suggests that weak aseismic slip (≤10 mm) on the plate-interface may produce significant (up to 25 kPa) stress perturbations capable of triggering large-magnitude ($M > 6$) earthquakes in the upper-plate, such as the one recorded in Zakynthos immediately after the 2018 transient.

3. Discussion

On October 25, 2018, a M_w 6.9 earthquake ruptured the western end of the HSS, south of Zakynthos Island (Figure 1a) (Chousianitis & Konca, 2019; Haddad et al., 2020; Mouslopoulou et al., 2020; Sokos et al., 2020) and across a region where the African-Eurasian plate-motion transitions from convergence to transform through distributed faulting (Figure 1a) (Konstantinou et al., 2017; Pérouse et al., 2012). The two SSEs which were reported to precede the 2018 Zakynthos Earthquake (Mouslopoulou et al., 2020) appear to have played a key role in initiating a tectonic unrest (2014–2015 SSE) beneath western Peloponnese and, eventually, triggering (2018 SSE) the M_w 6.9 Zakynthos Earthquake. Geodetic modeling shows that the two SSEs have similar slip distributions (Figure 2). The earlier SSE occurred mainly beneath western Peloponnese and east of the Island of Zakynthos, where there was also an increase in seismicity rates in the forearc (Figure 3b). The 2018 SSE, on the other hand, occurred at slightly shallower depths (beneath the Island of Zakynthos) and was associated with an increase in the seismicity rates in the future epicentral area (Figure 3b). Interestingly, ΔCFS modeling indicates that the Zakynthos Earthquake occurred in an area of positive ΔCFS while the inner wedge east of Zakynthos accommodated largely negative ΔCFS; these stress perturbations are in good agreement with the fluctuations observed in the seismicity rates (Figures 3 and 5). The westward (updip on the plate-interface) migration of the loci of slow-slip and of the associated microseismicity in the upper-plate, together with the stress perturbations detected through the ΔCFS modeling, collectively suggest the triggering of the October 25, 2018 M_w 6.9 event.

The triggering scenario is also supported by our dynamic Coulomb wedge analysis that highlights a mechanically fragile forearc that fails in response to small changes of the megathrust strength. This sensitivity of forearcs to small stress changes has been previously documented mainly within the context of large megathrust earthquakes, such as the 2010 M_w 8.8 Maule earthquake and the 2011 M_w 9 Tohoku-Oki earthquake, where large parts of the forearc became extensionally critical due to small static stress drops of a few MPa (e.g., Dielforder, 2017; Wang et al., 2019). SSEs are likely to alter the strength of the megathrust for the following reasons: (a) slow slip is thought to occur along weak segments of the megathrust that are characterized by near-lithostatic pore fluid pressures (Behr & Bürgmann, 2021) and (b) it has been experimentally shown that shear dilatancy during SSE can reduce the pore fluid pressure in the fault zone by a few tens of MPa, which would temporarily increase the megathrust strength (Samuelson et al., 2009). For example, a decrease in basal pore fluid pressures of ≤10 MPa would suffice to "push" the forearc from an extensionally critical state to a compressively critical state. Notably, the outer wedge west of Zakynthos Island experienced mainly normal faulting in the years before the Zakynthos earthquake (Mouslopoulou et al., 2020), suggesting that it was in an extensionally critical state, while the Zakynthos Earthquake and its aftershock sequence (Mouslopoulou et al., 2020) records transpression, indicating that the wedge became compressively critical just before the earthquake. However, the potential changes in megathrust friction due to the SSE remain difficult to constrain, because the actual physical processes that occur at depth along the plate-interface remain only partly understood (Behr & Bürgmann, 2021; Bürgmann, 2018).

The down-dip extent of the two SSEs modeled here (Figure 2) are expected to straddle the frictional-viscous transition along the plate-interface which is commonly controlled by the thermal conditions of the subducting slab and occurs at temperatures of ~350–500°C (Gao & Wang, 2017) and depths of 20–50 km (Dragert et al., 2001; Hirose et al., 1999; Schwartz & Rokosky, 2007; Wallace & Beavan, 2006). In Greece, however,

where the subducting slab of the HSS is very old (220–230 Ma) and cold, the isotherms of 350–500°C are located much deeper, at ~60–80 km depth (Halpaap et al., 2019; Speranza et al., 2012). We therefore propose that the down-dip extent of the SSEs is likely controlled here by the depth of the continental Aegean Moho, which lies at about 35–40 km beneath central Peloponnese (Gao & Wang, 2017; Halpaap et al., 2019). Further evidence from seismic tomography shows increased pore-fluid pressures beneath central Peloponnese due to fluids escaping from deep sections of the slab (>80 km) into the mantle wedge and shallower depths (<40 km) (Halpaap et al., 2018, 2019). High pore-fluid pressure on the plate-interface near the mantle wedge favors the occurrence of SSEs and deep tectonic tremor (Audet & Bürgmann, 2014; Gao & Wang, 2017). The latter, however, has not yet been detected along the HSS (Bocchini et al., 2021), perhaps because long-lived SSEs occurring near the down-dip limit of the seismogenic zone, as those detected beneath western Peloponnese, are not strongly correlated with tremor episodes (Obara & Kato, 2016).

In summary, we find that, although plate-motion along the Hellenic subduction occurs mostly (>80%) aseismically (Reilinger et al., 2010), long-term (i.e., several months) slow slip may characterize sections of the plate-interface zone where isolated patches remain strongly locked (Saltogianni et al., 2020). In circumstances where such slow-slip occurs within a mechanically fragile forearc, tectonic unrest with associated large-magnitude earthquakes, may be triggered. These findings may have implications for other weakly locked subduction systems worldwide, such as those encountered in central/northern Hikurangi in New Zealand, central Japan, Costa Rica, Ecuador, etc. (Davis et al., 2015; Ozawa et al., 2007; Shaddox & Schwartz, 2019; Vallée et al., 2013; Wallace & Beavan, 2010).

Data Availability Statement

The geodetic data used for the slow slip modeling are from Mouslopoulou et al. (2020). The earthquake catalog is included in Supporting Information S1 of this article (Data Set S1). For earthquake relocation, we used picks from the following seismic networks: HL (National Observatory of Athens) (NOA, 1997), HT (Aristotle University of Thessaloniki) (AUTH, 1981), HP (University of Patras) (UP, 2000), and HA (University of Athens) (UA, 2008). In Figure 1a, 11 focal mechanisms derived from the repository of the National Observatory of Athens (http://bbnet.gein.noa.gr/HL/seismicity/mts/revised-moment-tensors) and the offshore bathymetry from EMODnet (https://portal.emodnet-bathymetry.eu/?menu=19). Maps in figures in the main text and the Supporting Information S1 were produced using the Generic Mapping Tools (GMT) software available at https://www.generic-mapping-tools.org/ (last accessed July 2021).

Acknowledgments
The authors thank the staff of the Institute of Geodynamics of the National Observatory of Athens for data archiving/processing and all other partners of the HUSN (including the University of Patras, the University of Thessaloniki and the University of Athens) for publicly sharing the data. Simone Cesca (GFZ), Panos Psimoulis (University of Nottingham), and Michael Gianniou (HEPOS) are thanked for helpful discussions. Roland Bürgmann, an anonymous reviewer and Whitney Behr (Editor) are thanked for their constructive comments and efficient editorial handling, respectively. Open access funding enabled and organized by Projekt DEAL.

References

Audet, P., & Bürgmann, R. (2014). Possible control of subduction zone slow-earthquake periodicity by silica enrichment. *Nature*, *510*(7505), 389–392. https://doi.org/10.1038/nature13391

AUTH. (1981). *Aristotle University of Thessaloniki Seismological Network*. International Federation of Digital Seismograph Networks. https://doi.org/10.7914/SN/HT

Bedford, J., & Bevis, M. (2018). Greedy automatic signal decomposition and its application to daily GPS time series. *Journal of Geophysical Research: Solid Earth*, *123*(8), 6992–7003. https://doi.org/10.1029/2017JB014765

Behr, W. M., & Bürgmann, R. (2021). What's down there? The structures, materials and environment of deep-seated slow slip and tremor. *Philosophical Transactions of the Royal Society A: Mathematical, Physical and Engineering Sciences*, *379*(2193), 20200218. https://doi.org/10.1098/rsta.2020.0218

Bocchini, G. M., Brüstle, A., Becker, D., Meier, T., van Keken, P. E., Ruscic, M., et al. (2018). Tearing, segmentation, and backstepping of subduction in the Aegean: New insights from seismicity. *Tectonophysics*, *734–735*, 96–118. https://doi.org/10.1016/j.tecto.2018.04.002

Bocchini, G. M., Martínez-Garzón, P., Harrington, R. M., & Bohnhoff, M. (2021). Does deep tectonic tremor occur in the central-eastern Mediterranean basin? *Journal of Geophysical Research: Solid Earth*, *126*(1), 2020JB020448. https://doi.org/10.1029/2020JB020448

Bouchon, M., Durand, V., Marsan, D., Karabulut, H., & Schmittbuhl, J. (2013). The long precursory phase of most large interplate earthquakes. *Nature Geoscience*, *6*(4), 299–302. https://doi.org/10.1038/ngeo1770

Briole, P., Ganas, A., Elias, P., & Dimitrov, D. (2021). The GPS velocity field of the Aegean. New observations, contribution of the earthquakes, crustal blocks model. *Geophysical Journal International*, *226*(1), 468–492. https://doi.org/10.1093/gji/ggab089

Bürgmann, R. (2018). The geophysics, geology and mechanics of slow fault slip. *Earth and Planetary Science Letters*, *495*, 112–134. https://doi.org/10.1016/j.epsl.2018.04.062

Chousianitis, K., & Konca, A. O. (2019). Intraslab deformation and rupture of the entire subducting crust during the 25 October 2018 Mw 6.8 Zakynthos earthquake. *Geophysical Research Letters*, *46*(24), 14358–14367. https://doi.org/10.1029/2019GL085845

Cirella, A., Romano, F., Avallone, A., Piatanesi, A., Briole, P., Ganas, A., et al. (2020). The 2018 Mw 6.8 Zakynthos (Ionian Sea, Greece) earthquake: Seismic source and local tsunami characterization. *Geophysical Journal International*, *221*(2), 1043–1054. https://doi.org/10.1093/gji/ggaa053

Cochran, E. S., Vidale, J. E., & Tanaka, S. (2004). Earth tides can trigger shallow thrust fault earthquakes. *Science*, *306*(5699), 1164–1166. https://doi.org/10.1126/science.1103961

Cruz-Atienza, V. M., Tago, J., Villafuerte, C., Wei, M., Garza-Girón, R., Dominguez, L. A., et al. (2021). Short-term interaction between silent and devastating earthquakes in Mexico. *Nature Communications*, *12*(1), 2171. https://doi.org/10.1038/s41467-021-22326-6

Davis, E. E., Villinger, H., & Sun, T. (2015). Slow and delayed deformation and uplift of the outermost subduction prism following ETS and seismogenic slip events beneath Nicoya Peninsula, Costa Rica. *Earth and Planetary Science Letters*, *410*, 117–127. https://doi.org/10.1016/j.epsl.2014.11.015

Dielforder, A. (2017). Constraining the strength of megathrusts from fault geometries and application to the Alpine collision zone. *Earth and Planetary Science Letters*, *474*, 49–58. https://doi.org/10.1016/j.epsl.2017.06.021

Dixon, T. H., & Moore, J. C. (Eds.). (2007). *The seismogenic zone of subduction thrust faults* (p. 692). Columbia University Press.

Dmitrieva, K., Segall, P., & DeMets, C. (2015). Network-based estimation of time-dependent noise in GPS position time series. *Journal of Geodesy*, *89*(6), 591–606. https://doi.org/10.1007/s00190-015-0801-9

Dragert, H., Wang, K., & James, T. S. (2001). A silent slip event on the deeper Cascadia subduction interface. *Science*, *292*(5521), 1525–1528. https://doi.org/10.1126/science.1060152

Ganas, A., Briole, P., Bozionelos, G., Barberopoulou, A., Elias, P., Tsironi, V., et al. (2020). The 25 October 2018 Mw = 6.7 Zakynthos earthquake (Ionian Sea, Greece): A low-angle fault model based on GNSS data, relocated seismicity, small tsunami and implications for the seismic hazard in the west Hellenic Arc. *Journal of Geodynamics*, *137*, 101731. https://doi.org/10.1016/j.jog.2020.101731

Gao, X., & Wang, K. (2014). Strength of stick-slip and creeping subduction megathrusts from heat flow observations. *Science*, *345*(6200), 1038–1041. https://doi.org/10.1126/science.1255487

Gao, X., & Wang, K. (2017). Rheological separation of the megathrust seismogenic zone and episodic tremor and slip. *Nature*, *543*(7645), 416–419. https://doi.org/10.1038/nature21389

Habermann, R. E. (1981). Precursory seismicity patterns: Stalking the mature seismic GAP. In *Earthquake prediction* (pp. 29–42). American Geophysical Union (AGU). https://doi.org/10.1029/ME004p0029

Haddad, A., Ganas, A., Kassaras, I., & Lupi, M. (2020). Seismicity and geodynamics of western Peloponnese and central Ionian Islands: Insights from a local seismic deployment. *Tectonophysics*, *778*, 228353. https://doi.org/10.1016/j.tecto.2020.228353

Halpaap, F., Rondenay, S., & Ottemöller, L. (2018). Seismicity, deformation, and metamorphism in the Western Hellenic Subduction Zone: New constraints from tomography. *Journal of Geophysical Research: Solid Earth*, *123*(4), 3000–3026. https://doi.org/10.1002/2017JB015154

Halpaap, F., Rondenay, S., Perrin, A., Goes, S., Ottemöller, L., Austrheim, H., et al. (2019). Earthquakes track subduction fluids from slab source to mantle wedge sink. *Science Advances*, *5*(4), eaav7369. https://doi.org/10.1126/sciadv.aav7369

Hamling, I. J., & Wallace, L. M. (2015). Silent triggering: Aseismic crustal faulting induced by a subduction slow slip event. *Earth and Planetary Science Letters*, *421*, 13–19. https://doi.org/10.1016/j.epsl.2015.03.046

Harris, R. A. (1998). Introduction to special section: Stress triggers, stress shadows, and implications for seismic hazard. *Journal of Geophysical Research: Solid Earth*, *103*(B10), 24347–24358. https://doi.org/10.1029/98JB01576

Heki, K., Miyazaki, S., & Tsuji, H. (1997). Silent fault slip following an interplate thrust earthquake at the Japan Trench. *Nature*, *386*(6625), 595–598. https://doi.org/10.1038/386595a0

Hirose, H., Hirahara, K., Kimata, F., Fujii, N., & Miyazaki, S. (1999). A slow thrust slip event following the two 1996 Hyuganada earthquakes beneath the Bungo Channel, southwest Japan. *Geophysical Research Letters*, *26*(21), 3237–3240. https://doi.org/10.1029/1999GL010999

King, G. C. P., Stein, R. S., & Lin, J. (1994). Static stress changes and the triggering of earthquakes. *Bulletin of the Seismological Society of America*, *84*(3), 935–953.

Konstantinou, K. I., Mouslopoulou, V., Liang, W.-T., Heidbach, O., Oncken, O., & Suppe, J. (2017). Present-day crustal stress field in Greece inferred from regional-scale damped inversion of earthquake focal mechanisms. *Journal of Geophysical Research: Solid Earth*, *122*(1), 506–523. https://doi.org/10.1002/2016JB013272

Lamb, S. (2006). Shear stresses on megathrusts: Implications for mountain building behind subduction zones. *Journal of Geophysical Research: Solid Earth*, *111*(B7). https://doi.org/10.1029/2005JB003916

Langbein, J. (2008). Noise in GPS displacement measurements from Southern California and Southern Nevada. *Journal of Geophysical Research: Solid Earth*, *113*(B5). https://doi.org/10.1029/2007JB005247

Mann, P., & Frohlich, C. (1999). Classification and tectonic comparison of subduction to strike-slip transitions on active plate boundaries. *Subduction to strike-slip transitions on plate boundaries. Penrose Conference, Puerto Plata, Dominican Republic*.

Marsan, D., & Wyss, M. (2011). *Seismicity rate changes*. https://doi.org/10.5078/CORSSA-25837590

Matthews, M. V., & Reasenberg, P. A. (1988). Statistical methods for investigating quiescence and other temporal seismicity patterns. *Pure and Applied Geophysics*, *126*(2), 357–372. https://doi.org/10.1007/BF00879003

Mazzotti, S., & Adams, J. (2004). Variability of near-term probability for the next great earthquake on the Cascadia subduction zone. *Bulletin of the Seismological Society of America*, *94*(5), 1954–1959. https://doi.org/10.1785/012004032

Mouslopoulou, V., Bocchini, G.-M., Cesca, S., Saltogianni, V., Bedford, J., Petersen, G., et al. (2020). Earthquake-swarms, slow-slip and fault-interactions at the western-end of the Hellenic Subduction System precede the Mw 6.9 Zakynthos earthquake, Greece. *Geochemistry, Geophysics, Geosystems*, *21*(12), e2020GC009243. https://doi.org/10.1029/2020GC009243

Mouslopoulou, V., Saltogianni, V., Nicol, A., Oncken, O., Begg, J., Babeyko, A., et al. (2019). Breaking a subduction-termination from top to bottom: The large 2016 Kaikōura Earthquake, New Zealand. *Earth and Planetary Science Letters*, *506*, 221–230. https://doi.org/10.1016/j.epsl.2018.10.020

NOA. (1997). *Institute of Geodynamics, National Observatory of Athens Seismic Network*. International Federation of Digital Seismograph Networks. https://doi.org/10.7914/SN/HL

Obara, K., & Kato, A. (2016). Connecting slow earthquakes to huge earthquakes. *Science*, *353*(6296), 253–257. https://doi.org/10.1126/science.aaf1512

Ohta, Y., Freymueller, J. T., Hreinsdóttir, S., & Suito, H. (2006). A large slow slip event and the depth of the seismogenic zone in the south central Alaska subduction zone. *Earth and Planetary Science Letters*, *247*(1), 108–116. https://doi.org/10.1016/j.epsl.2006.05.013

Okada, Y. (1985). Surface deformation due to shear and tensile faults in a half-space. *Bulletin of the Seismological Society of America*, *75*(4), 1135–1154. https://doi.org/10.1785/bssa0750041135

Ozawa, S., Suito, H., & Tobita, M. (2007). Occurrence of quasi-periodic slow-slip off the east coast of the Boso peninsula, Central Japan. *Earth, Planets and Space*, *59*(12), 1241–1245. https://doi.org/10.1186/BF03352072

Peng, Z., & Gomberg, J. (2010). An integrated perspective of the continuum between earthquakes and slow-slip phenomena. *Nature Geoscience*, *3*(9), 599–607. https://doi.org/10.1038/ngeo940

Pérouse, E., Chamot-Rooke, N., Rabaute, A., Briole, P., Jouanne, F., Georgiev, I., & Dimitrov, D. (2012). Bridging onshore and offshore present-day kinematics of central and eastern Mediterranean: Implications for crustal dynamics and mantle flow. *Geochemistry, Geophysics, Geosystems*, *13*(9). https://doi.org/10.1029/2012GC004289

Radiguet, M., Cotton, F., Vergnolle, M., Campillo, M., Walpersdorf, A., Cotte, N., & Kostoglodov, V. (2012). Slow slip events and strain accumulation in the Guerrero gap, Mexico. *Journal of Geophysical Research: Solid Earth*, *117*(B4). https://doi.org/10.1029/2011JB008801

Reasenberg, P. A., & Simpson, R. W. (1992). Response of regional seismicity to the static stress change produced by the Loma Prieta earthquake. *Science*, *255*(5052), 1687–1690. https://doi.org/10.1126/science.255.5052.1687

Reilinger, R., McClusky, S., Paradissis, D., Ergintav, S., & Vernant, P. (2010). Geodetic constraints on the tectonic evolution of the Aegean region and strain accumulation along the Hellenic subduction zone. *Tectonophysics*, *488*(1), 22–30. https://doi.org/10.1016/j.tecto.2009.05.027

Saltogianni, V., Mouslopoulou, V., Oncken, O., Nicol, A., Gianniou, M., & Mertikas, S. (2020). Elastic fault interactions and earthquake rupture along the southern Hellenic subduction plate interface zone in Greece. *Geophysical Research Letters*, *47*(13), e2019GL086604. https://doi.org/10.1029/2019GL086604

Samuelson, J., Elsworth, D., & Marone, C. (2009). Shear-induced dilatancy of fluid-saturated faults: Experiment and theory. *Journal of Geophysical Research: Solid Earth*, *114*(B12). https://doi.org/10.1029/2008JB006273

Scholz, C. H. (1998). Earthquakes and friction laws. *Nature*, *391*(6662), 37–42. https://doi.org/10.1038/34097

Schwartz, S. Y., & Rokosky, J. M. (2007). Slow slip events and seismic tremor at circum-Pacific subduction zones. *Reviews of Geophysics*, *45*(3). https://doi.org/10.1029/2006RG000208

Segall, P., & Bradley, A. M. (2012). Slow-slip evolves into megathrust earthquakes in 2D numerical simulations. *Geophysical Research Letters*, *39*(18). https://doi.org/10.1029/2012GL052811

Shaddox, H. R., & Schwartz, S. Y. (2019). Subducted seamount diverts shallow slow slip to the forearc of the northern Hikurangi subduction zone, New Zealand. *Geology*, *47*(5), 415–418. https://doi.org/10.1130/G45810.1

Sokos, E., Gallovič, F., Evangelidis, C. P., Serpetsidaki, A., Plicka, V., Kostelecký, J., & Zahradník, J. (2020). The 2018 Mw 6.8 Zakynthos, Greece, earthquake: Dominant strike-slip faulting near subducting slab. *Seismological Research Letters*, *91*(2A), 721–732. https://doi.org/10.1785/0220190169

Speranza, F., Minelli, L., Pignatelli, A., & Chiappini, M. (2012). The Ionian Sea: The oldest in situ ocean fragment of the world? *Journal of Geophysical Research: Solid Earth*, *117*(B12). https://doi.org/10.1029/2012JB009475

UA. (2008). *Hellenic Seismological Network, University of Athens, Seismological Laboratory*. International Federation of Digital Seismograph Networks. https://doi.org/10.7914/SN/HA

Uchida, N., Iinuma, T., Nadeau, R. M., Bürgmann, R., & Hino, R. (2016). Periodic slow slip triggers megathrust zone earthquakes in northeastern Japan. *Science*, *351*(6272), 488–492. https://doi.org/10.1126/science.aad3108

UP. (2000). *University of Patras, Seismological Laboratory*. International Federation of Digital Seismograph Networks. https://doi.org/10.7914/SN/HP

Vallée, M., Nocquet, J.-M., Battaglia, J., Font, Y., Segovia, M., Régnier, M., et al. (2013). Intense interface seismicity triggered by a shallow slow slip event in the Central Ecuador subduction zone. *Journal of Geophysical Research: Solid Earth*, *118*(6), 2965–2981. https://doi.org/10.1002/jgrb.50216

Wallace, L. M., Barnes, P., Beavan, J., Dissen, R., Litchfield, N., Mountjoy, J., et al. (2012). The kinematics of a transition from subduction to strike-slip: An example from the central New Zealand plate boundary. *Journal of Geophysical Research*, *117*. https://doi.org/10.1029/2011JB008640

Wallace, L. M., & Beavan, J. (2006). A large slow slip event on the central Hikurangi subduction interface beneath the Manawatu region, North Island, New Zealand. *Geophysical Research Letters*, *33*(11). https://doi.org/10.1029/2006GL026009

Wallace, L. M., & Beavan, J. (2010). Diverse slow slip behavior at the Hikurangi subduction margin, New Zealand. *Journal of Geophysical Research: Solid Earth*, *115*(B12). https://doi.org/10.1029/2010JB007717

Wang, K., Brown, L., Hu, Y., Yoshida, K., He, J., & Sun, T. (2019). Stable forearc stressed by a weak megathrust: Mechanical and geodynamic implications of stress changes caused by the M = 9 Tohoku-Oki earthquake. *Journal of Geophysical Research: Solid Earth*, *124*(6), 6179–6194. https://doi.org/10.1029/2018JB017043

Wang, K., & Hu, Y. (2006). Accretionary prisms in subduction earthquake cycles: The theory of dynamic Coulomb wedge. *Journal of Geophysical Research: Solid Earth*, *111*(B6). https://doi.org/10.1029/2005JB004094

Wang, L., Wang, R., Roth, F., Enescu, B., Hainzl, S., & Ergintav, S. (2009). Afterslip and viscoelastic relaxation following the 1999 M 7.4 İzmit earthquake from GPS measurements. *Geophysical Journal International*, *178*(3), 1220–1237. https://doi.org/10.1111/j.1365-246X.2009.04228.x